NATIONAL ADVISORY COMMITTEE FOR AERONAUTICS

TECHNICAL NOTE 4052

TWO FACTORS INFLUENCING TEMPERATURE DISTRIBUTIONS AND THERMAL STRESSES IN STRUCTURES

By William A. Brooks, Jr., George E. Griffith, and H. Kurt Strass

Langley Aeronautical Laboratory
Langley Field, Va.

Washington

June 1957

NATIONAL ADVISORY COMMITTEE FOR AERONAUTICS

TECHNICAL NOTE 4052

TWO FACTORS INFLUENCING TEMPERATURE DISTRIBUTIONS AND THERMAL STRESSES IN STRUCTURES

By William A. Brooks, Jr., George E. Griffith, and H. Kurt Strass

SUMMARY

The influence of joint conductivity and internal radiation on temperature distribution and thermal stresses has been discussed. Joints of poor conductivity can occur in normal fabrication procedure and greatly alter temperature distributions and increase thermal stresses. On the other hand, internal radiation tends to make the temperature distributions more uniform and thereby relieves thermal stress.

INTRODUCTION

Thermal stresses are unquestionably an important consideration in the design of supersonic aircraft. Such stresses are usually produced by nonuniform temperature distributions - the greater the temperature variation within the structure, the larger the thermal stresses. The present paper deals briefly with two factors which may affect the temperature distribution, and thus the thermal stresses, within a structure; these two factors are joint conductivity and internal radiation. In order to indicate some of the effects of these two factors without unnecessary structural complications, the basic structure considered consists of a length of skin with an integral or an attached web. In addition to theoretical results, experimental data were obtained by heating the structure either aerodynamically or by laboratory radiant-heat sources.

SYMBOLS

α	coefficient of thermal expansion
c	specific heat
E	modulus of elasticity

ϵ	emissivity
h	heat-transfer coefficient
h_j	joint conductivity coefficient
k	thermal conductivity
M	Mach number
q	heating rate
t	skin thickness
T	temperature
T_0	initial temperature
T_1	maximum skin temperature
T_2	minimum web temperature
T_{aw}	equilibrium temperature
τ	time
w	specific weight
σ	thermal stress

Subscripts:

RC	radiation and conduction
C	conduction
MAX	maximum

DISCUSSION

Simple Integral Structure

Consider first the simplest possible type of skin-web combination, one without joints and without internal radiation effects. Figure 1 shows such a structure, a symmetrical integral H-section with a flange (or skin) of thickness t symmetrically heated at a constant rate q;

within this structure heat transfer takes place by conduction only. The actual temperature T minus the initial temperature T_0, multiplied by the material thermal conductivity k and divided by the heating rate q and skin thickness t, is plotted against a time parameter in which τ is the elapsed time, c the specific heat, and w the specific weight. The choice of these dimensionless parameters makes it possible to present on the same plot the results for a given cross section of different materials subjected to different heating rates. The calculated results, shown by the solid lines, are obtained by a simple analysis assuming constant material thermal properties and no heat losses. Point 1, which is farthest from the heat sink afforded by the web, will be the hottest point in the structure, whereas point 2, which is farthest from the heat source, will be the coolest. As a consequence of assuming no heat losses and a constant heat input, the average temperature of the structure is proportional to the mass of the section and varies linearly with time. In order to check the theory, three tests were made involving constant heating rates of 5, 16, and 41 Btu/ft^2-sec. Each test is represented by a different symbol, and the experimental temperatures are plotted for various times until the maximum skin temperature reached 450° F. The parameters are such that the data for the highest heating rate, shown by the diamonds, appear at the extreme lower end of the curves, whereas the data for the lowest heating rate extend the full length of the curves. The test results are in fairly good agreement with the theory; any discrepancy is due largely to the assumption of constant thermal properties used in the theory.

At any point in the structure, the thermal stress is proportional to the difference between the average temperature and the temperature of the point in question. When multiplied by the appropriate material properties, these differences can be converted into thermal stresses, such as shown in figure 2.

In this figure thermal-stress distributions are shown for both the low and high heating rates of 5 and 41 Btu/ft^2-sec for the times when the maximum skin temperature reached 450° F. The skin stresses appear in region A and the web stresses, in region B. The solid lines represent thermal stresses calculated from measured temperatures shown in figure 1, and the symbols represent experimental stresses obtained from strain-gage readings corrected for differential expansion between the gage and specimen. The agreement between theory and experiment is quite good. As would be expected, the higher heating rate allows less time for heat to be conducted into the web, thus provides larger temperature differences in the structure, and consequently yields larger thermal stresses. For the heating rate of 41 Btu/ft^2-sec the maximum skin stress, shown at the extreme right, and the maximum web stress, at the extreme left, are more than twice the values shown for the rate of 5 Btu/ft^2-sec, despite the fact that the skin temperature rise was the same.

Another significant point is that the maximum stresses are not related in the same proportion as the heating rates, which have an 8 to 1 ratio. The stresses shown here are those which existed when the skin temperature T_1 was 450° F. If, however, the skin temperature were not limited to 450° F and a comparison were made at the same value of time, then, indeed, the stresses would be proportional to the heating rate.

It is also possible to present the stresses in a dimensionless form as was done for the temperatures. Figure 3 shows the dimensionless thermal stresses at various times during the progress of the three tests at heating rates of 5, 16, and 41 Btu/ft^2-sec. It is again evident that the high-heating-rate data are grouped at the lower end of the theoretical curves which are represented by the solid lines, whereas the data for the low heating rate extend the full length of the curves. The theoretical stresses are obtained by using the theoretical temperatures of figure 1. The agreement between theory and experiment is about the same as that in figure 1, and any discrepancy is due to the same reason.

The results of these three figures indicate that fairly accurate temperatures and stresses can be predicted in a simple integral structure where only conductive heat transfer need be considered and, further, that strain-gage readings, if treated properly, can give reasonable stress results. However, if this structure had contained any joints, greater temperature differences would have resulted, and accurate calculations would have become somewhat more difficult.

Structure With Attached Webs

In order to show some of the effects of joints, the temperatures in one skin-web combination of a multiweb wing, a more realistic aircraft-type structure which contains riveted joints, will be examined. When six 20-inch-chord, multiweb wings identical in cross section - that is, with the same overall size, skin thickness, material, and so forth - were tested at sea-level conditions at a Mach number of 2 in a blowdown jet, the results were as shown in figure 4. This figure shows the temperature difference $T_1 - T_2$ between the maximum temperature in the skin (point 1) and the minimum web temperature (point 2) divided by the maximum possible skin temperature rise $T_{aw} - T_0$ plotted against time. The upper dot-dash curve gives the theoretical temperature-ratio drop if no heat is conducted into the web, that is, if the joint conductivity h_j is equal to zero, and the lower dot-dash curve gives the theoretical results for perfect joint conductivity. The experimental data for five of the wings, indicated by the shaded area, lie close to the curve for perfect joint conductivity. On the other hand, the data for the sixth wing show that the increased temperature drop is somewhat closer to the curve for no joint conductivity. Since the temperature distribution depends mainly

upon heat conduction within the structure, this increased temperature difference can be attributed almost solely to a lower joint conductivity. The much poorer thermal conductivity of the joints of the one wing, compared with the other five wings, was not obtained by design but rather results from the small variations in otherwise identical structures expected from normal fabrication techniques. The 50-percent increase in temperature drop of the one wing over the average of the other five wings also resulted in a substantial increase in thermal stress. In fact, the wing with the largest temperature drop fluttered and then suffered a dynamic failure; whereas, the one wing among the other five which was identical in every detail survived its test without damage. Construction details, such as the inclusion of ribs, invalidate further comparison with the other models. However, it seems obvious that joint conductivity can have an important, and sometimes adverse, effect on the temperature variation in a structure and hence on the thermal stresses and, as a result, on the structural integrity.

In figure 5 the maximum nondimensional temperature drops have been plotted against a dimensionless joint conductivity parameter $h_j t/k$ where h_j is the thermal conductivity of the joint. Calculated results are shown by the solid lines. In the calculations the value of 0.013 for ht/k, the Biot number (an index of the rate of external to internal heat transfer), was determined by the experimental aerodynamic heat-transfer coefficient h. The symbols indicate data obtained from the tests and show a 6 to 1 variation in h_j which apparently can be expected even from good shop practice. Data obtained by Barzelay, Tong, and Holloway (refs. 1 and 2) cover an even wider range in h_j. Although a considerable scatter in h_j is shown by the five lowest test points, these points are in good agreement with the theory since they lie in a region where a fairly large change in joint conductivity has little effect on the temperature drop. Thus, the band for the five wings shown in figure 4 masks a considerable variation in h_j. The sixth point, which does not show such good agreement, is in a region where a small change in h_j can alter the temperature drop appreciably. The spread of h_j within the band shown in figure 4 is of the same order of magnitude as the variation from the top of the band to the curve for the one wing.

If the maximum skin or web stress were plotted instead of the temperature drop, a similar variation with $h_j t/k$ could be observed - the lower the value of h_j, the higher the thermal stress, as evidenced by the failure of the one wing.

Actual flight-test results are shown in figure 6 for a duplicate of one of the five wings which had very good joint conductivity. The Mach number and altitude for the flight are shown at the top of the figure. The temperature difference $T_1 - T_2$ between the skin and the web

center line is plotted against time. When this wing was attached to a rocket model, the results were as shown by the solid line, which lies much closer to the calculated curve for $h_j = 300$ Btu/ft^2-hr-$^\circ$F than to the curve for perfect joint conductivity. Since a value of $h_j = 300$ would lie slightly to the left of the test point for the one wing with the largest temperature difference shown in figure 5, the joints of this wing would be considered poor from the standpoint of thermal conductivity. In this case failure of the wing was prevented by the inclusion of a chordwise rib.

Internal Radiation in an Integral Structure

As was mentioned previously, the effect of joints is to increase the magnitude of the thermal stresses. However, if the temperatures involved are sufficiently high, it is possible that internal radiation in a structure may bring about some thermal-stress relief. The hotter parts of the structure transfer heat to the cooler parts by radiation and thereby lessen the temperature differences. Although there is an increased interest in this phenomenom, very little information can be found on this subject.

Therefore, in order to evaluate some of the effects of internal radiation on the temperature distribution within a multicell beam, such as shown in figure 7, an analog solution was made to determine the temperature distribution of an infinitely long box whose internal surfaces have an emissivity of 1. The procedure was to assume a constant rate of heat input until the maximum skin temperature reached a prescribed limit and then to maintain this skin temperature while the web temperature approached the skin temperature.

Heat was put into both skins at the rate of 5 Btu/ft^2-sec until the maximum skin temperature T_1 reached 1,200° F, at which time the skin temperature was kept constant. The maximum skin temperature T_1 and the minimum web temperature T_2 are plotted against time in seconds. The dashed lines are the solution when internal radiation is neglected; the solid lines represent the case when radiation is included. In this situation it can be seen that, when radiation is included, steady state is reached much more rapidly than when conduction only is considered. It can also readily be seen that the maximum temperature difference between the skin and the web, when conduction and radiation are considered, occurs at approximately 75 seconds and is about two-thirds of that when conduction only is considered.

In order to make a preliminary survey, other heating rates and skin-temperature levels were also investigated as shown in figure 8. Here,

in order to show one of the effects of internal radiation, the ratio of the maximum difference between skin temperature and web temperature for both radiation and conduction to the maximum difference for conduction only is plotted against the skin temperature T_1. For a given heating rate, the ratio of the temperature differences will approach a minimum value as the skin temperature increases. In the case of $q = 1$ Btu/ft^2-sec, the limit is nearly reached at a skin temperature of 1,200° F. The curve for the highest heating rate will eventually reach the lowest limit but at a temperature far in excess of 1,200° F. For the conditions in the figure, radiation effects are most significant when heating rates are low and temperatures are high.

Figure 9 shows some preliminary experimental results. The specimen was made of $\frac{1}{16}$-inch Inconel with the cross section as shown ($2\frac{1}{2}$-inch-square cells) and was 12 inches long. The emissivity of the internal surfaces was about 0.8. The heating rates were approximately 5 and $2\frac{1}{2}$ Btu/ft^2-sec. Although there is a measurable reduction in the maximum temperature difference, the reduction is not as large as indicated by the idealized theoretical results.

CONCLUDING REMARKS

In summary, two factors, joint conductivity and internal radiation, which influence temperature distribution and therefore thermal stresses, have been discussed. Even normal fabrication techniques can produce joints of such poor conductivity as to cause the temperature differences to increase markedly over those of an integral structure. On the other hand, at the higher temperatures internal radiation has the effect of making the temperature differences less severe and the thermal stresses smaller. At the higher temperatures these two effects tend to cancel one another.

Langley Aeronautical Laboratory,
National Advisory Committee for Aeronautics,
Langley Field, Va., March 6, 1957.

REFERENCES

1. Barzelay, Martin E., Tong, Kin Nee, and Holloway, George F.: Effect of Pressure on Thermal Conductance of Contact Joints. NACA TN 3295, 1955.

2. Barzelay, Martin E., Tong, Kin Nee, and Holloway, George F.: Thermal Conductance of Contacts in Aircraft Joints. NACA TN 3167, 1954.

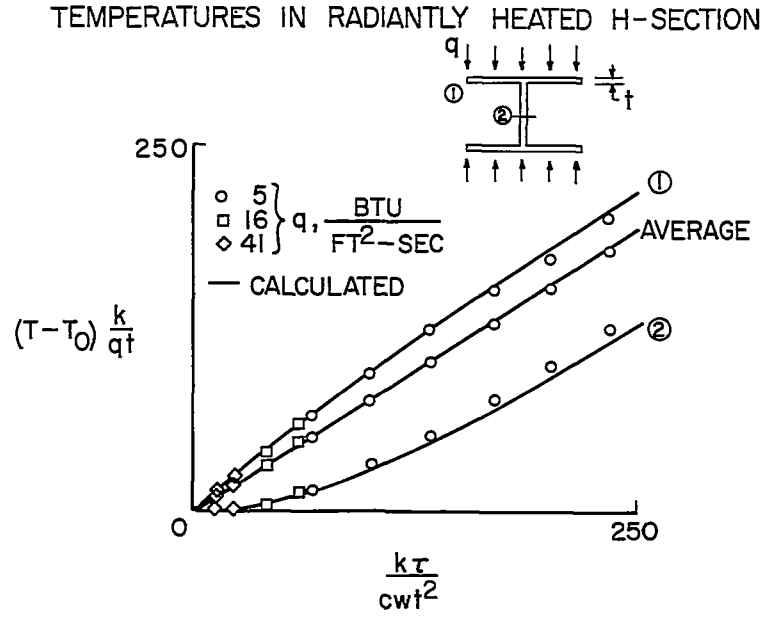

Figure 1

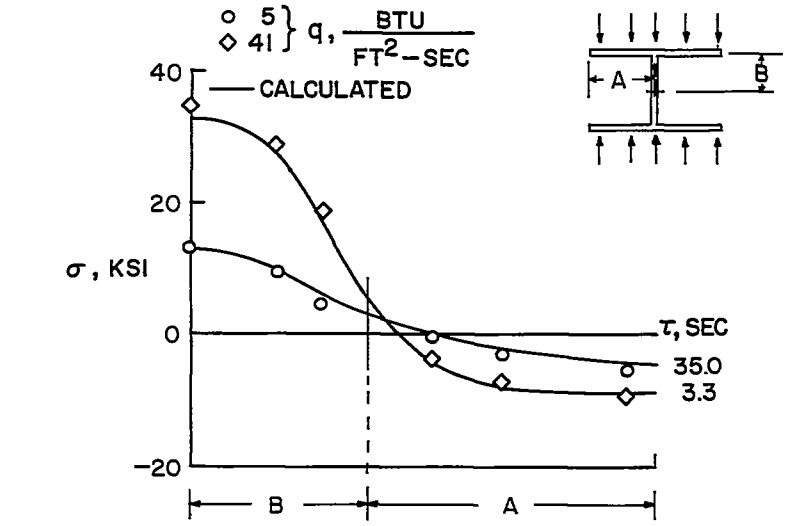

Figure 2

THERMAL STRESSES IN RADIANTLY HEATED H-SECTION

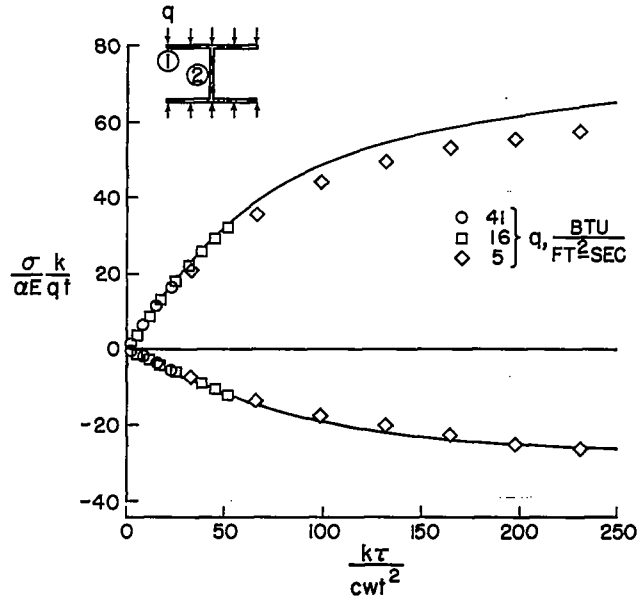

Figure 3

TEMPERATURE DIFFERENCES IN 6 MULTIWEB WINGS

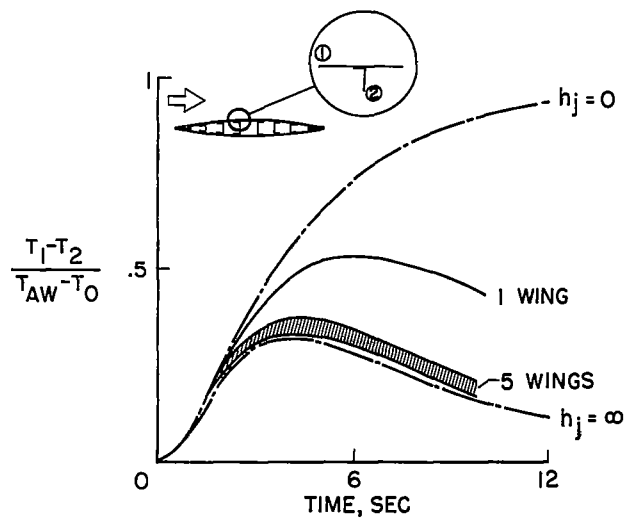

Figure 4

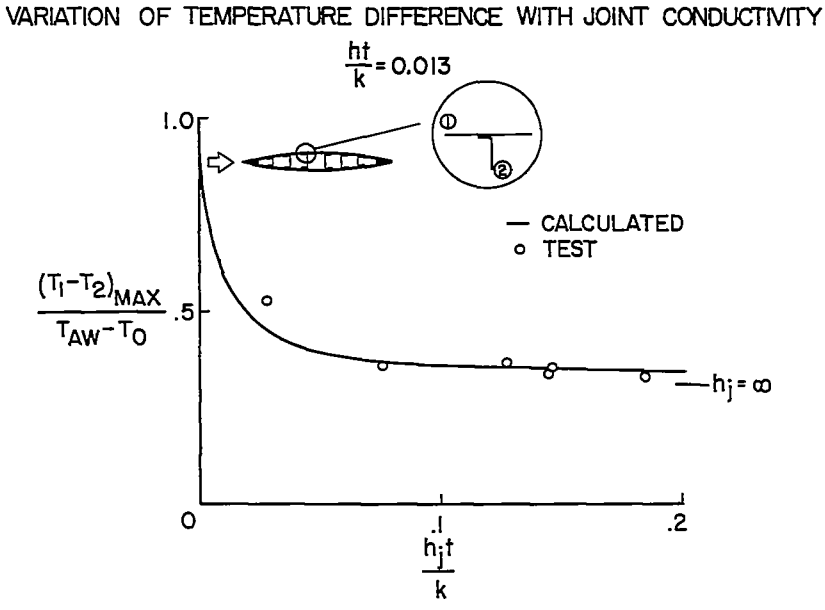

Figure 5

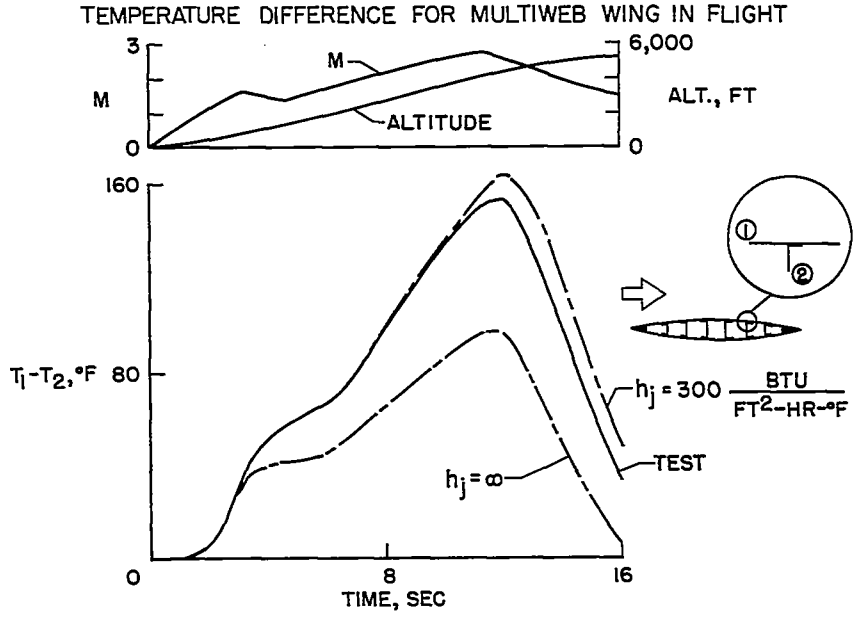

Figure 6

TEMPERATURE HISTORIES FOR BOX BEAM WITH INTERNAL RADIATION

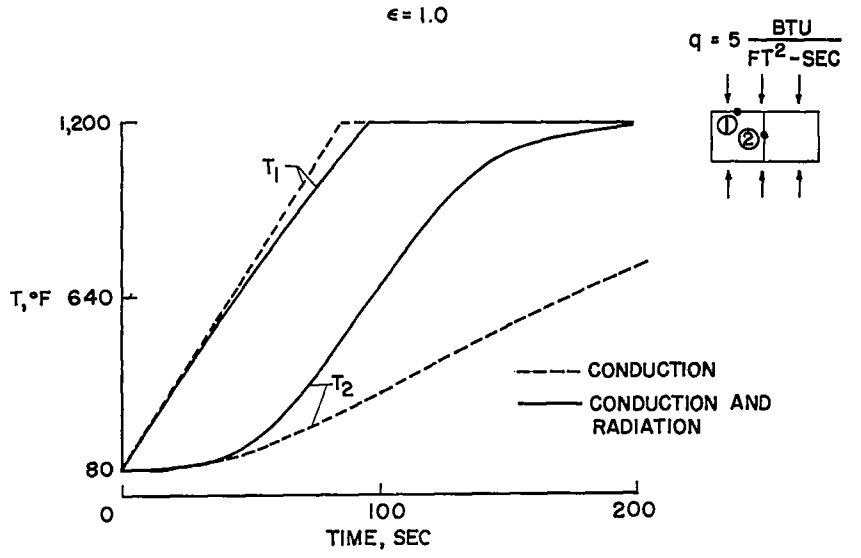

Figure 7

INTERNAL RADIATION EFFECTS FOR VARIOUS HEATING RATES

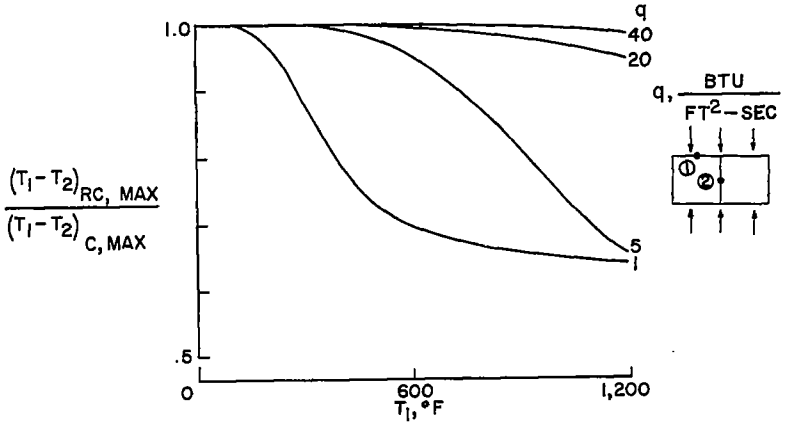

Figure 8

EXPERIMENTAL RESULTS FOR INTERNAL RADIATION

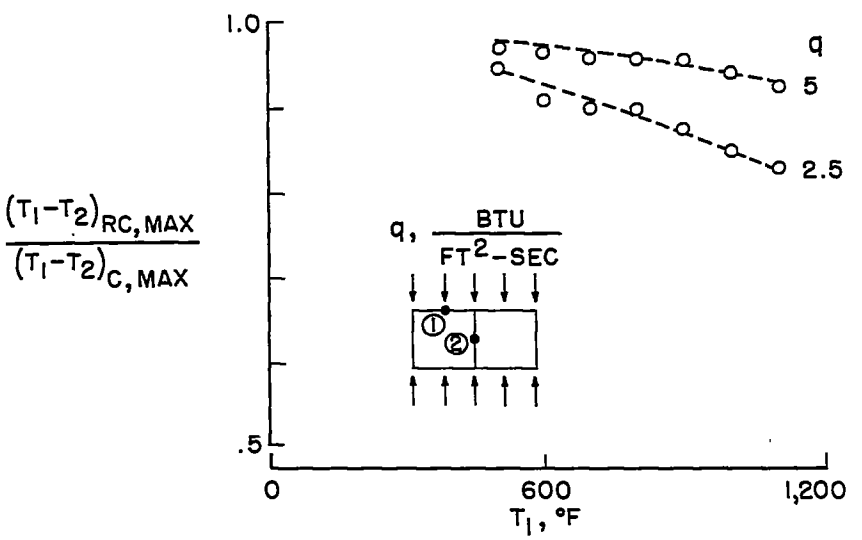

Figure 9